

Uni-axial and bending test for the determination of fracture properties of fiber reinforced concrete

A. Meda

Department of Civil Engineering, University of Brescia, Italy.

G.A. Plizzari

Department of Engineering Technologies and Design, University of Bergamo, Italy.

L. Sorelli

Department of Civil Engineering, University of Brescia, Italy.

ABSTRACT: Steel fiber reinforcement allows to enhance the fracture performance in concrete. The concrete toughness can be increased by adding one or more types of fibers to the concrete matrix. In order to evaluate the fiber effect on the material and the structural response, adequate tests have to be carried out. Fracture properties of concrete reinforced with a combination of fibers with different length is analyzed herein by means of uni-axial and bending tests. Experimental results on specimens reinforced with a low fiber content can be affected by a remarkable scatter: for this reason, an assumption based on the number of fibers expected in the cracked surface was introduced in order to identify a representative curve for each test and each material. A numerical simulation based on non-linear fracture mechanics of the experimental test was carried out in order to better identify the fiber contribution in the fracture propagation.

Keywords: fiber reinforced concrete, hybrid fibers, uni-axial tests, bending tests.

1 INTRODUCTION

After the pioneer work of Romualdi & Batson (1963) and more than 30 years of intensive research (Shah & Rangan 1971), Steel Fiber Reinforced Concrete (SFRC) is nowadays extensively used in structures where the reinforcement is not essential for integrity and safety (especially for slabs on grade and for shotcrete in tunnels). However, in recent years fibers have been used as principal reinforcement in structures under bending and shear (Meda et al. 2002, Di Prisco et al. 2003).

Steel fibers mainly enhance concrete toughness and fibers of different geometries or material properties have different effects on concrete behavior. Based on the idea to take simultaneously advantages of the effects of different types of fibers, new materials called Hybrid FRCs have been developed by combining fibers of different material properties and geometries (Banthia et al. 2000, Banthia & Nandakumar 2003). As an example, Lawler et al. (2002) showed that a combination of fibers of different lengths improves both resistance and permeability of the composite. Also from the mere mechanical point of view, synergistic effects were observed on the pull-out strength of a single (long) steel fiber from a cementitious matrix reinforced with short steel fibers (Markovich et al. 2002).

Aim of the present work is to investigate the possibility of optimizing concrete toughness by combining steel fibers of different lengths. Concrete toughness was determined by means of both uni-axial and bending tests on notched specimens. Freely rotating platens with spherical hinges were adopted as boundary conditions in the uni-axial tests to better control the crack development. Bending tests were carried out on beam specimens having two different geometries and different crack length/beam depth ratios. One of the beam geometries has the same fracture surface of the uni-axial specimens to better study the strain gradient effects.

After completing an experimental program presented elsewhere (Meda et al. 2003), numerical tests based on FE elements and fracture mechanics are here presented. Numerical simulations allow the determination of a good approximation of the post-cracking strength based on a poly-linear law.

The possibility of adopting bi-linear or tri-linear fracture law has been studied in the presence of one fiber or different fibers reinforcement. In fact, since fibers of different lengths become efficient at different stages of the cracking process, the micro-fibers control the micro-crack growth while the macro-fibers become active for larger crack openings.

2 EXPERIMENTAL TESTS

2.1 Materials

All the specimens adopted in the research were made of a normal strength concrete whose composition is illustrated in Table 1. A grain size distribution close to the Bolomey curve was adopted for the aggregates whose maximum diameter size was equal to 15 mm.

Two different types of steel fibers were used: the first one had a length of 30 mm and a diameter of 0.6 mm (aspect ratio = 50) while the second one was a shorter fiber having a length of 12 mm and a diameter of 0.18 mm (aspect ratio = 67); these fibers will be named in the following as “macro-fiber” and “micro-fiber” respectively. Table 2 shows the geometrical and mechanical characteristics of the fibers used in the present research-work.

Fibers were added to the concrete matrix in four different combinations as shown in Table 3 but the volume fraction of fibers was maintained equal to 0.38% in all cases.

The specimens were cured in a fog room until the time of the test and a vaseline layer was applied on the crack section in order to avoid shrinkage cracking.

Table 1. Composition of the concrete matrix.

CEM II/A-LL 32.5 R	355 kg
Water	180 l
Supelastizer	3.9 l
Aggregates	1900 kg
Water/cement ratio	0.55

Quantities for 1 m³.

Table 2. Properties of the steel fibers.

	macro-fiber	micro-fiber
Length	30 mm	12 mm
Diameter	0.60 mm	0.18 mm
Aspect ratio	50	67
Yielding strength	1100 MPa	1800 MPa
Young's modulus	210 GPa	210 GPa

Table 3. Fiber combinations.

	Plain	Micro	Macro	Hybrid
Micro-fiber	0%	0%	0.38%	0.19%
Macro-fiber	0%	0.38%	0%	0.19%
Total fiber content	0%	0.38%	0.38%	0.38%

2.2 Experimental set-up

In order to investigate the fiber effects on concrete behavior, fracture tests should be performed and a stable control of the test is necessary. For this reason, a 500 kN hydraulic testing machine (Instron) with a PID closed loop control that permits to compensate the finite stiffness of the load system was adopted.

Uni-axial tests with freely rotating platens were performed on specimen having a size of 100x200x40 mm (Fig. 1a) that were sawed from concrete prisms having a size of 310x100x40 mm to favor a three dimensional distribution of fibers. A single notch with a depth of 15 mm, a width of 4 mm and a tip with a triangular shape was sawn with a diamond blade.

Four Linear Variable Differential Transformers (LVDTs) with a gage length of 45 mm were located across the notched section to evaluate the relative displacement and rotation of the sections at each side of the crack surface (Fig. 1). In order to reduce undesired eccentricities, the specimens were carefully positioned (and then glued) on steel platens by adopting four micrometers with a precision of 0.01 mm; this allowed to obtain a good alignment of the specimen along the loading axis. The free rotation of the platens was allowed by two spherical hinges placed at a distance of 150 mm from the glued surface; this allowed to localize the center of rotation at the specimen ends.

The Crack Mouth Opening Displacement (CMOD), measured by a Clip Gauge, was adopted as feedback signal. The CMOD rate was 1 μ m/min until the load-displacement curve had passed the peak. Afterwards, the CMOD rate was set to 2 μ m/min. Although it includes the elastic deformations of concrete, the average value of the displacement measured by the two LVDTs astride the notch was conventionally assumed as the Crack Tip Opening Displacement (CTOD; Fig. 1a).

In addition to the uniaxial tensile tests, four point bending tests were performed on specimens having two different sizes. The first one was a beam of 150x150x600 mm with a 45 mm depth notch and it was tested according to the Italian Standard (UNI 2003; Fig. 2a). The second one employed the same crack length/beam depth ratio as the uni-axial tensile test specimen to study the strain gradient effects (Slowik & Wittmann 1992). These beams had a size of 100x320x40 mm and were tested with a span length of 300 mm and a distance between the load points of 100 mm (Fig. 2b).

Three LVDTs were adopted to measure the vertical displacement at mid-span and under the load points while two LVDTs were placed at the notch

tip to measure the CTOD. Finally, a clip gauge, placed across the notch to measure the CMOD (Fig. 2), was used as feed-back signal. The CMOD rate was 50 $\mu\text{m}/\text{min}$ for the larger beams (UNI 2003) and 2.5 $\mu\text{m}/\text{min}$ for the smaller beams.

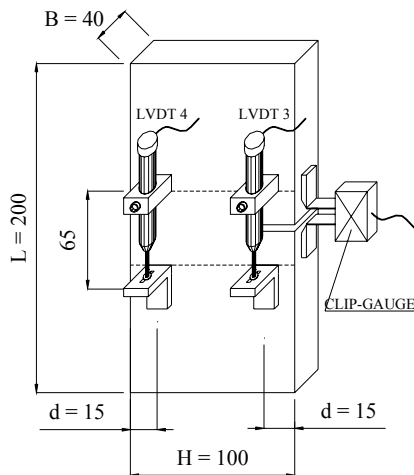


Figure 1. Specimen geometry and instrument positions for the uni-axial test (measure in mm).

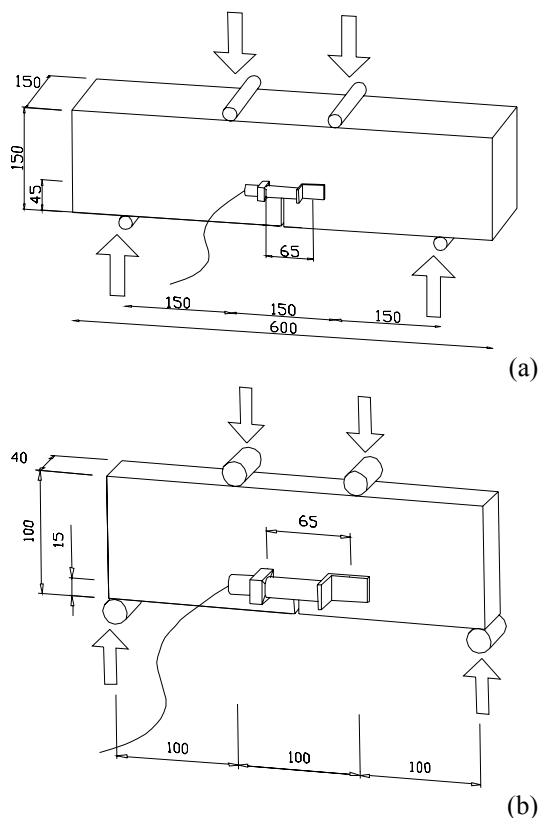


Figure 2. Four point bending test: specimen geometry for larger (a) and smaller (b) beams.

2.3 Experimental results

The experimental results are presented in Figure 3 in terms of nominal stress (σ_N) versus CTOD. The nominal stress is determined by assuming a linear stress distribution in the resistant part of the notched section. At least four specimens for each material and each specimen geometry were tested.

Experimental results from FRC with low fiber contents are very sensitive to the number of fibers in the cracked section that shows a larger scatter in small surface areas. For the sake of comparison, only one representative curve for each material is exhibited in Figure 4 by choosing specimens having a fiber density (number of fibers per unit area in the cracked section) close to the average value (0.38%).

It should be observed that fiber geometry markedly changes the concrete toughness while the peak stress ($\sigma_{N,max}$) is slightly influenced by presence of macro-fibers (Fig. 4). The micro-fibers increase the peak and the post cracking strength for small crack openings but this residual strength rapidly decreases since fibers are quickly pulled-out from the matrix (Meda et al. 2003). On the contrary, macro-fibers become efficient for larger crack openings since they require larger displacements to be active. In the Hybrid FRC, the residual strength is enhanced for both smaller and larger crack openings.

3 NUMERICAL TESTS

All the experimental tests were simulated by adopting Non-Linear Fracture Mechanics (NLFM) with Merlin (Reich et al. 1994) that is based on a discrete crack approach.

The aim of the numerical tests was to define a poly-linear stress-crack opening law ($\sigma-w$) for the post cracking behavior of each material. Fracture of plain concrete or concrete reinforced with a single type of fiber is often approximated with a bilinear law where the first steeper branch simulates the bridging of the early microcracks while the second branch simulates the aggregate interlocking in plain concrete or the fiber links in FRC (Wittmann et al., 1988; Fig. 5). When more than one type of fibers is adopted, it may be necessary to use more branches since different fibers may activate at different crack openings. In the present work, where microfibers were added to macrofibers, a trilinear law may be useful since microfibers activate before macrofibers (Fig. 5).

By using the post-cracking laws representative of each material, it should be possible to simulate all

the three types of test. The chosen procedure aimed to define the post cracking law through the simulation of the uni-axial tensile test (that is closer to the pure tensile behavior) and subsequently use the same law for simulating both the bending tests.

The FE mesh was based on elastic triangular elements (plane stress) and interface elements with zero thickness in the fracture sections (whose position is known because of the notch) to simulate a fictitious crack. The interface elements link rigidly the elastic elements until the maximum tensile strength is reached. Eventually, they transmit a stress that is function of the crack opening.

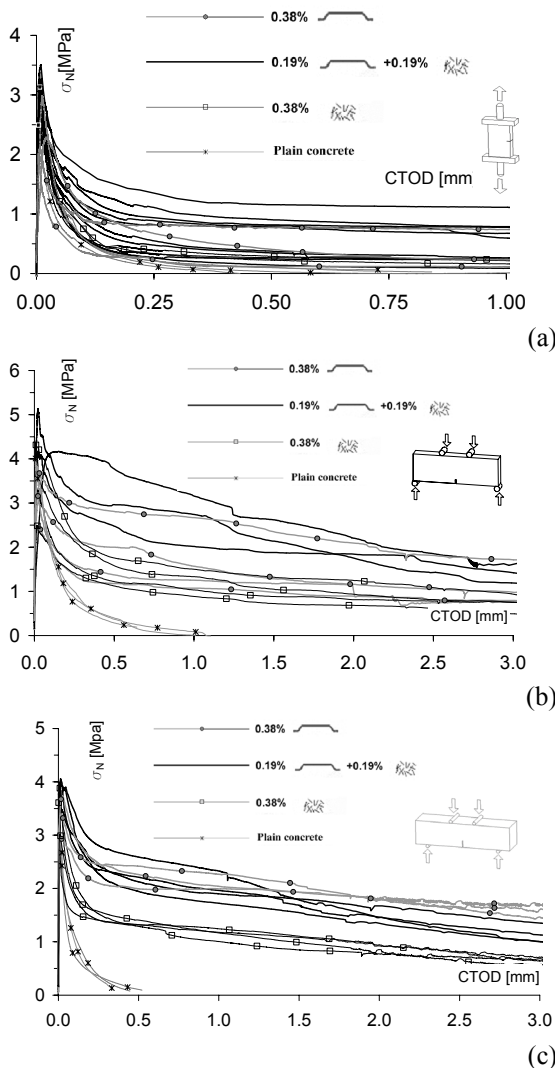


Figure 3. Nominal stress versus CTOD for uni-axial tensile tests (a), small bending tests (b) and large bending tests (c).

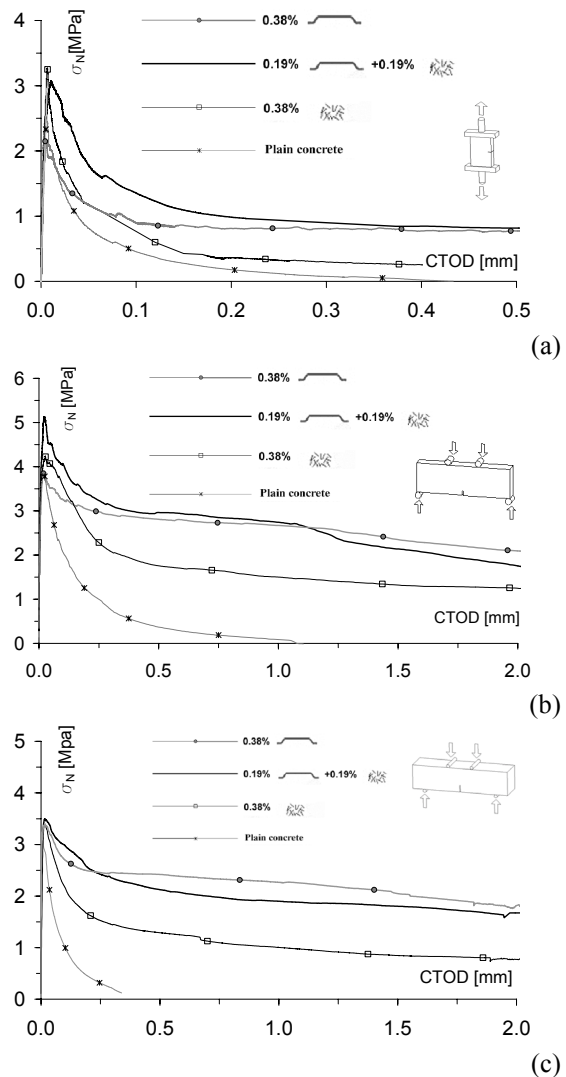


Figure 4. Typical σ_N -CTOD curves from uni-axial tensile tests (a), small bending tests (b) and large bending tests (c).

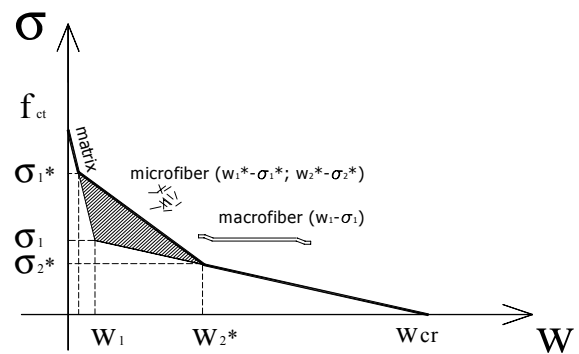


Figure 5. Approximation of the softening law by a bi-linear or tri-linear curve.

The uni-axial tensile tests were modeled by adopting 1522 three-node triangular elements (plane stress) for the elastic sub-domains, linked by means of 94 interface elements. (Fig. 6a). The hinges of the steel platens of the numerical model were placed in the same position of the experimental ones. The large and small bending specimens were respectively modeled with 2280 and 3016 triangular elements (plane stress); with 34 and 47 interface elements respectively (Figs. 6b, c).

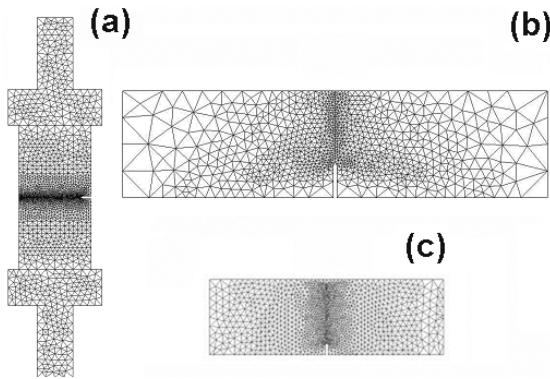


Figure 6. FE Meshes of the tensile specimen with the steel plates (a), large beam specimens (b) and small beam specimens (c).

Table 4. Constitutive parameters for the σ -w law (*tri-linear relationship).

	f_{ct} (MPa)	σ_1 (Mpa)	w_1 (mm)	σ_2 (MPa)	w_2 (mm)	w_{cr} (mm)
Plain concrete	2.89	0.55	0.018	-	-	0.18
Macro-FRC	2.89	0.90	0.016	-	-	50
Micro-FRC	2.89	0.47	0.0285	-	-	3
Hybrid-FRC*	2.89	1.20	0.015	0.5	0.50	50

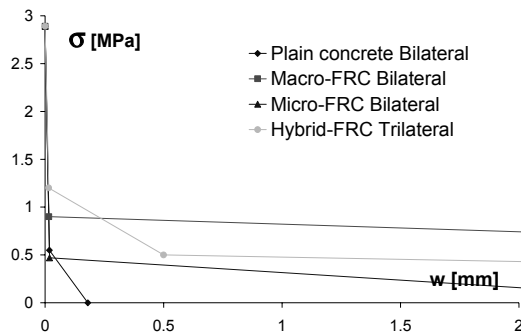


Figure 7. Stress-crack opening curves determined from the best-fitting procedure.

In the numerical analyses, the modulus of elasticity ($E_c=25127$ MPa) was experimentally determined on cylindrical specimens ($\phi=100$ mm and $h=200$ mm). The tensile strength (f_{ct}) was determined from the experimental compressive strength according to the CEB Model Code 90 (CEB 1993).

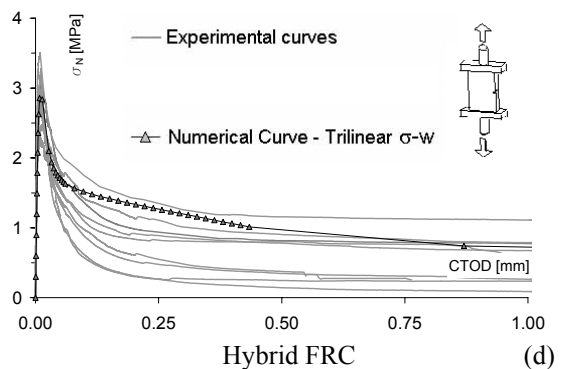
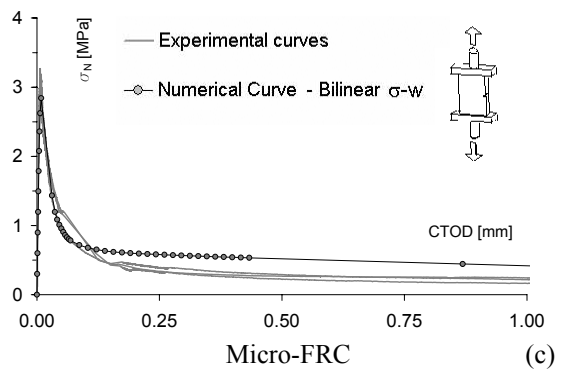
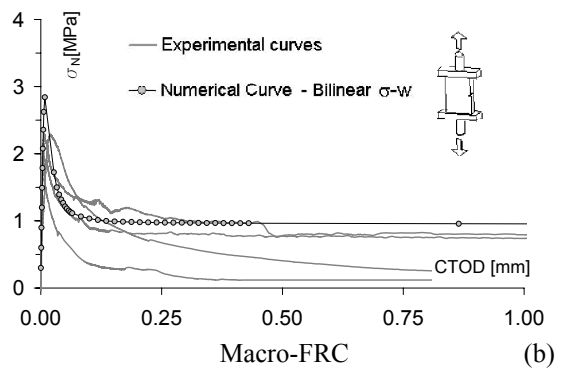
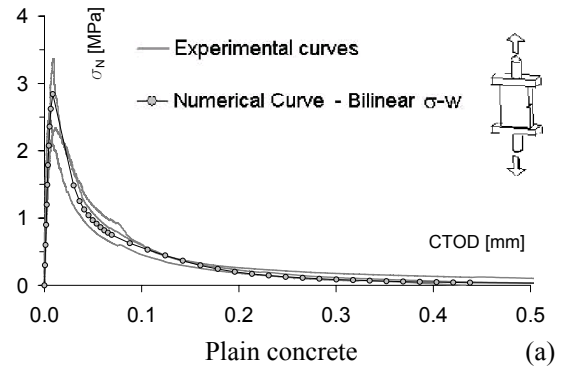


Figure 8. Experimental and numerical nominal stress (σ_N) versus CTOD curves from uni-axial tensile tests.

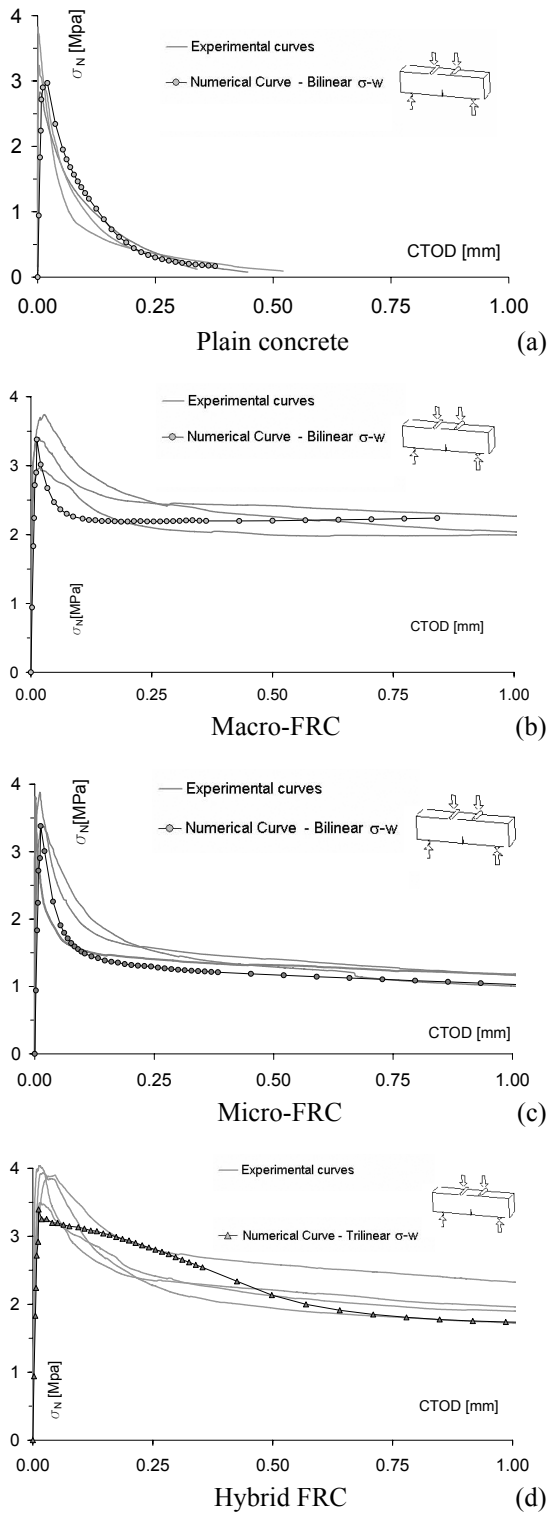


Figure 9. Experimental and numerical nominal stress versus CTOD for plain concrete (a), macro-FRC (b), micro-FRC (c) and hybrid FRC (d) from bending tests on large specimens.

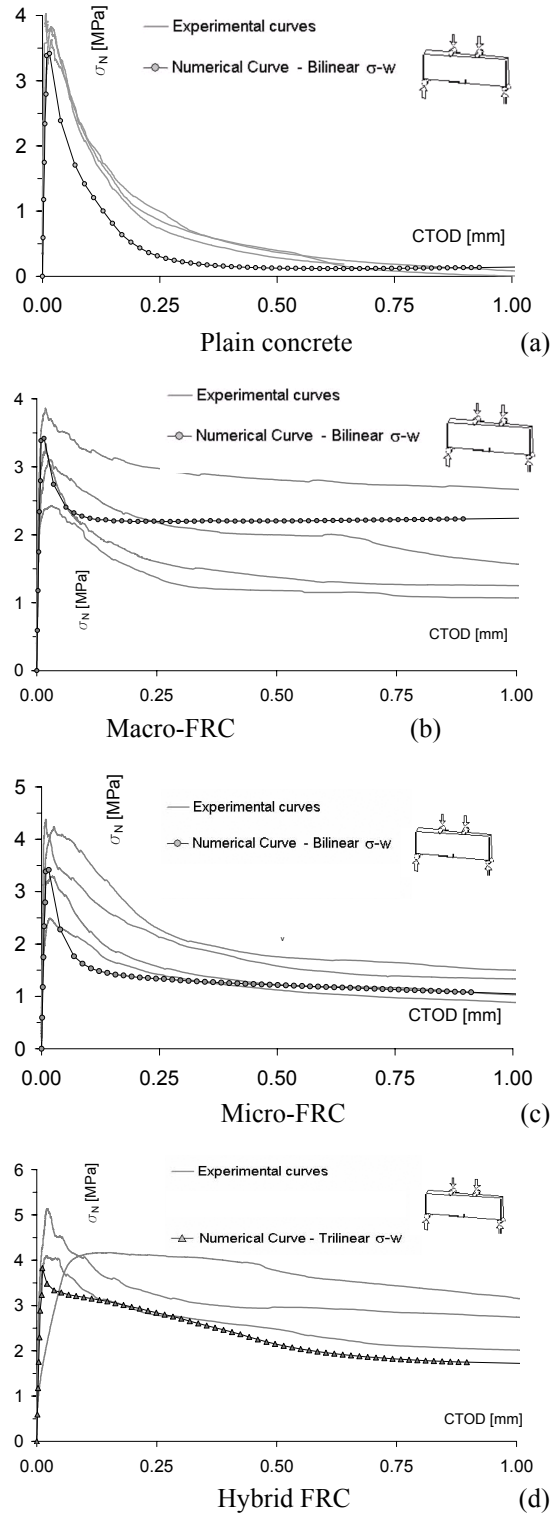


Figure 10. Experimental and numerical nominal stress versus CTOD for plain concrete (a), macro-FRC (b), micro-FRC (c) and hybrid FRC (d) from bending tests on small specimens.

As mentioned above, the parameters of the σ - w law (Tab. 4) were determined by means of a best fitting procedure (Roelfstra & Wittmann 1986) on the tensile test response. The parameters of the poly-linear laws that provided the best fitting of the experimental curves (from uni-axial tests) are summarized in Table 4 and plotted in Figure 7. One should observe that the first steeper branch of the post-cracking laws is the same for all the materials; this is consistent with the assumption that the initial branch of the post-cracking curves characterizes the bridging of the concrete matrix between the early micro-cracks and it is mainly due to the concrete matrix (which is the same for all the materials adopted; Wittmann et al., 1988).

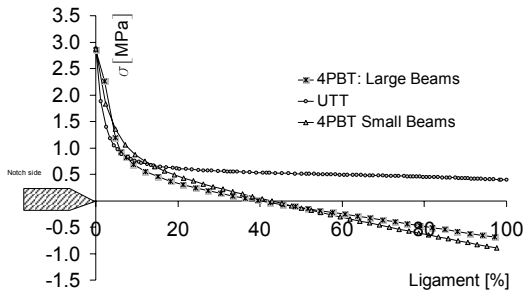


Figure 11. Stress distribution along the ligament for small beams, large beams and tensile specimens at crack onset (Hybrid FRC).

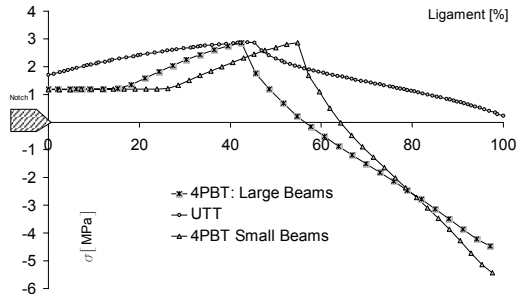


Figure 12. Stress distribution along the ligament in the case of small beams, large beams and tensile specimens at Peak load (Hybrid FRC).

The numerical curves of the stress (σ_N) versus crack tip opening displacement (CTOD) from uni-axial tensile tests are plotted with the experimental curves in Figure 8. It can be noticed that a bilinear law allows for a good fitting of the experimental results from all the materials. FRC with hybrid-fibers is well approximated by a tri-linear curve since micro-fibers start activating before the macro ones (Fig. 8d).

By adopting the same softening law defined for the uni-axial tensile test, bending tests on both large (Fig. 9) and small (Fig. 10) specimens have

been simulated. One should notice that the softening laws determined from uni-axial tensile tests provide a fairly good approximation of fracture behavior of both small and large beams under bending.

The numerical results also provide information on the stresses distribution along the fictitious crack (fracture section). Figures 11 and 12, that concern hybrid FRC specimens, show the stress distribution at the crack onset and at the peak load respectively. One should note that, both at the crack-onset and at the peak load, the stress distribution that can be obtained with uni-axial tensile tests is more uniform. At peak load, the overall section is nearly in pure tension (Fig. 12).

4 CONCLUDING REMARKS

Experimental results from fracture tests carried out on normal strength concrete with a volume fraction of 0.38% of steel fibers are presented. The fibers have different geometries and are combined to obtain hybrid composites. Both bending tests and uni-axial tensile tests with freely rotating platens were performed on notched specimens.

In order to obtain a complete characterizations of fracture behavior of concrete reinforced with a low fiber content, adequate tests are needed; furthermore, particular care should be devoted to the specimen preparation and in the tests control in order to limit the scatter due in the testing procedure.

Experimental results are very sensitive to the strain gradient in the cracked section, to the fiber geometry and to the area of the cracked surface. In fact, a larger scatter of the experimental results was observed in specimens with a smaller cracked surfaces where a larger scatter in the density of macro-fiber was observed. On the contrary, a smaller scatter of the post-cracking curves was observed in specimens with micro-fibers only. However, the addition of micro fibers slightly reduces the dispersion in the results that characterizes the mechanical behavior of FRC with a low content of macro-fibers.

Hybrid combination of short and long steel fibers can also improve concrete toughness for both small and large crack opening displacements. This benefit can be useful for the serviceability state and fatigue. In addition, other synergic effects from the combination of micro and macro fibers are due to other effects (i.e. reduction of shrinkage cracking) not considered in the present experimental program.

A numerical simulation based on Non-Linear Fracture Mechanics of the experimental tests was carried out in order to better understand the material properties in terms of post-cracking response (σ -w). The numerical results show that the post-cracking softening law determined from uni-axial tensile tests provides a fairly good approximation of the flexural behavior of both small and large beams.

Post-cracking behavior (σ -w curve) can be defined by means of bilinear law when a single type of fiber is adopted; on the contrary, FRC with hybrid fibers is better approximated by a tri-linear law that takes into account the different behavior of micro and macro-fibers. In fact, smaller fibers start activating before larger fibers.

Numerical analyses also provide the stress distribution on the crack surface and show that the uni-axial tensile test better simulates fracture behavior of concrete (i.e. at the peak load, the stress distribution along the cracked section is more uniform).

REFERENCES

- Banthia, N. & Nandakumar, N. 2003. Crack Growth Resistance of Hybrid Fiber Composites. *Journal of Cement Composites (UK)*, 25(1): 3-9.
- Banthia, N., Bindiganavile, V & Yan, C. 2000. Development and Application of High Performance Hybrid Fiber Reinforced Concrete, In *Fifth RILEM International Symposium on Fiber Reinforced Concrete (BEFIB2000)*, Lyon, France, 13-15 September 2000: pp 471-480. Bagnex (France): RILEM.
- CEB 1993. Model Code 90. *CEB Bulletin*, 213-214.
- Di Prisco M, Iorio, F. & Plizzari, G.A. 2003. HPSFRC prestressed roof elements, in Test and Design Methods for Steel Fibre Reinforced Concrete - Background and Experiences. In B. Schnütgen and L. Vandewalle (eds.), *Proceedings of the RILEM TC 162-TDF Workshop*, Bochum (Germany), 20-21 March 2003: 161-188. Bagnex (France): RILEM.
- Lawler, J.S., Zampini, D., & Shah, S.P. 2002. Permeability of Cracked Hybrid Fiber-Reinforced Mortar under Load. *ACI Materials Journal*, 94: 379-385.
- Markovich, I., Van Mier, J.G.M. & Walraven, J.C. 2002. Single fiber from the hybrid fiber reinforced matrices. In *International Symposium on High Strength/High Performance Concrete*, Leipzig (Germany), 16-20 June, 2002: 1175-1186.
- Meda, A., Minelli, F., Plizzari, G.A. & Failla, C. 2002. Experimental study on shear behaviour of prestressed SFRC beams. In *International Symposium on High Strength/High Performance Concrete*, Leipzig (Germany), 16-20 June, 2002: 369-382.
- Meda, A., Plizzari, G.A., Sorelli & L. Banthia. 2003. Uni-axial and bending tests on hybrid fibre reinforced concrete. IN *Celebrating Concrete: People and Practice*, Dundee (UK). 3-4 September 2003: pp. 709-718.
- Roelfstra, P.E. & Wittmann, F.H. 1986. Numerical Method to Link Strain Softening with Failure of Concrete. In F.H. Wittmann (ed), *Fracture Toughness and Fracture Energy*: 163-175. Amsterdam: Elsevier.
- Reich, R. W., Cervenka, J. & Saouma, V. E. 1994. *Merlin, A three-dimensional finite element program based on a mixed-iterative solution strategy for problems in elasticity, plasticity, and linear and nonlinear fracture mechanics*. Palo Alto: EPRI. <http://civil.colorado.edu/~saouma/Merlin>.
- Romualdi, J. P. & Batson, G B. 1963. Mechanics of crack arrest in concrete beam with closely spaced reinforcement. *Journal of the American Institute*, 60: 775-789.
- Shah, S.P. & Rangan, B.V. 1971. Fibre reinforced concrete properties. *ACI Journal Proceedings*, 68(2): 126-134.
- Slowik, V. & Wittmann, F.H. 1992. Influence of Strain Gradient on Fracture Energy. In Z.P. Bazant (ed.) *FraMCoS-1*, Breckenridge (USA), June 1992: 424-429. Elsevier Applied Science: London.
- UNI 11039. 2003. *Steel fibre reinforced concrete - Part I: Definitions, classification specification and conformity - Part II: test method for measuring first crack strength and ductility indexes*. Italian Board for Standardization.
- Wittmann, F.H., Rokugo, K., Brühwiler, E., Mihashi, H., & Simonin, P. 1988. Fracture Energy and Strain Softening of Concrete as Determined by Means of Compact Tension Specimens, *Materials and Structures*, 21, 21-32.

ACKNOWLEDGEMENTS

The longer fibers were provided by Maccaferri (Bologna, Italy) while the shorter fibers were provided by La Matassina (Isola Vicentina, VI, Italy).

The Authors would also like to thank Mr Andrea Del Barba and the technicians of the laboratory of testing materials of the University of Brescia.

A special acknowledgement goes to Ing. Paolo Martinelli for the assistance in performing the experiments and in reducing data.